

Statistical Study of Coronal Mass Ejections during Rising Phase of Solar Cycle 24

Nisha Patel¹, Ajaysinh K. Jadeja²

¹Sir P. T. Sarvajanik College of Science, Surat-395 001, India

Shri J J T University, Rajsthan. – 333 001, India

²Gujarat Ayurved University, Jamnagar-361 008, India

Abstract: We have analyzed the data for more than 8000 CMEs which were obtained by Large Angle and Spectrometric Coronagraph Experiment on board Solar and Heliospheric Observatory during the rising phase of solar cycle 24. We found that the speed distribution for events with strong peak at $v = 344$ km/s and a long tail (>1000 km/s) is to a good approximation they can be fitted with a single log-normal distribution. Based on SOHO/LASCO catalogue and solar geophysical data, we have also studied the geo-effectiveness, solar source and flare association of a set of 192 halo CMEs during the period of 2008 to 2013. CMEs with maximum rate of geo-effectiveness occurred in maximum phase of solar cycle. Maximum number of strong storms occurred towards western hemisphere. Front disk halos are faster. Most intense storms are due to front side limb halo. Severe storms ($Dst < -200$ nT) not have been observed during the initial phase of solar cycle 24.

Keyword: Coronal Mass Ejection, Limb Halo, Disk Halo, SOHO, LASCO

1. Introduction

Coronal mass ejections (CMEs) are a topic of extensive study. In the late 1960s and early 1970s, white-light coronagraph observations from the Skylab space station and OSO-7 satellite had provided the opportunity to measure the speeds of CMEs directly (MacQueen et al., 1974; Brueckner, 1974). One of the main solar phenomena is CME ejected from the Sun. Earth-directed CMEs are very important, since they can produce geomagnetic storms. Usually these CMEs are seen as Halo CMEs (Howard et al., 1982). The relation between CMEs and the other phenomena has been examined by many researches (e.g., Gopalswamy et al., 2005, 2009; Gosling et al., 1976). Earlier measurements of the CMEs speeds have helped to advance our knowledge of the physical processes in the solar corona.

In observational point of view halo CMEs are classified as (i) full (type F), (ii) Asymmetric (type A) and (iii) partial (type P) halos [1]. F and A-type halos are having the apparent (sky plane) width 360 deg., while P-type halos are those with width greater than or equal to 120 deg. F and A-type halos are basically referred to as Halo CMEs. Extensive observations from the Solar and Heliospheric Observatory (SOHO) mission's Large Angle and Spectrometric Coronagraphs (LASCO) have shown that the full halos constitute ~ 3.6% of all CMEs, while CMEs with width ≥ 120 account for ~11% [2]. Frontside halo CMEs are further divided into Disk halos and Limb halos. Halos with their sources within 45 deg of the central meridian (longitudinal distance from the disk centre 45 deg.) are known as Disk halos while those with a central meridian distance beyond 45 deg and up to 90 deg are known as Limb halos. (Gopalswamy et al.)

There have been many researchers [3], [4] who have studied on the geo-effectiveness of halo CMEs using different samples. They found that ~75% of the front side halos produced significant geomagnetic storms. Gopalswamy et al. (2007) analyzed 378 halos for the period of 1996-2005 and

concluded that ~71% of Front side halos are geo-effective. Zhao and Webb used the same criteria of halo CMEs (width = 360deg) and found similar geo-effectiveness rates, while Kim et al and Yermolaev and Yermolaev defined their halos as CMEs with width 120 deg. and reported the lower geo-effectiveness rate.

Gopalswamy et al. [2007] showed that the geo-effectiveness (as shown by the Dst index) of a halo CME declines with increasing distance of its source region from the central meridian. Gopalswamy et al. [2010d] examined the IP counterparts of the 17 halo CMEs with source longitudes >45 (labeled as "limb halo CMEs" in that paper) and associated with intense (i.e., $Dst < -100$ nT) geomagnetic storms in the 1996–2005 period and They provide evidence that those geomagnetic storms are due to the sheath portion of the interplanetary CMEs (ICMEs). Moreover, they show that some of these storms are associated with interacting halo CMEs.

2. Data and Method

In this paper, we analyze the statistical properties of more than 8000 events by utilizing data from the catalogue of SOHO/LASCO CMEs. We compared statistical distributions against observed speed distributions. We have also analysed the geo-effectiveness, solar source and flare association of a set of 192 halo CMEs during the period of 2008 to 2013 (initial phase of solar cycle 24).

3. Speed distribution of CME

We used more than 8000 CMEs data observed by SOHO/LASCO from 2008 to 2013. For each event, the catalog contains height-time plots, plane of the sky speeds and the corresponding accelerations. The CME speeds are determined from both linear and quadratic fit to the height-time measurements. In our study we analyzed the linear (constant speed) fit which is preferable for 90% of the CMEs (Gopalswamy et al.) Figure-1 shows the distribution of the

number of CMEs, N against their speeds. A strong peak at 344 km/s and a long tail (>1000 km/s) to a good approximation that they can be fitted with a single log-normal distribution. We had also tried to find out correlation between parameters related to CME among them angular width of the CME and CME speed shows good correlation. Using selection criteria for angular width $> 45^\circ$, scattered Plot of angular width (w) vs speed (v) of CME shows correlation between w and v with correlation coefficient $r = 0.40245$. (Figure-2)

4. Source Identification and Flare Sizes

For source identification and flare sizes we used Hinode Flare Catalog (http://st4a.stelab.nagoya-u.ac.jp/hinode_flare/), which is maintained by ISAS/JAXA and Solar-Terrestrial Environment Laboratory, Nagoya University. For flares that do not have their solar source location listed, we also made use of daily movies obtained by the Extreme Ultraviolet Imager (EUVI) on board the Solar Terrestrial Relations Observatory (STEREO) in 195A to check if a source is front sided or back sided.

We identified that 85 halos originated from sources on the disk and we designated them as Front-side Full Halo (FFH). The remaining 107 halos were deemed back-sided because no activity could be found on the disk. We further divided the FFH- frontside- halos into disk halos (longitudinal distance from the disk centre $< 45^\circ$) and limb halos (longitudinal distance from the disk centre $> 45^\circ$) (Gopalswamy et al.(2007)). There were 35 disk halos and 50 limb halos. 59 of the 107 backside halos may also be considered as limb events based on the EUV dimming signatures seen above one limb where the CME first appears, but we do not know how far behind the limb the sources are. We refer these as backside limb (B-limb) halos as opposed to the frontside (F-limb) ones.

5. Geomagnetic Activity

For each halo CME, we obtained the minimum Dst value from the World Data Center in Kyoto (<http://swdcd.db.kugi.kyoto-u.ac.jp/dstdir/>) during a 4-5 days interval after the CME onset. We chose this interval because CMEs are known to reach Earth over this timescale [Gopalswamy et al., 2000]. Occasionally, CMEs take less than a day to reach Earth (Gopalswamy et al. 2005] for two cases in which the CME-driven shocks arrived at Earth in <19 hours). Since halo CMEs are faster on the average, they should arrive sooner than the slow solar wind does, but we use a wider window include some slow halos and allow for the fact that the geo-effective magnetic structure may be contained in the rear section of some ICMEs. Thus we expect the minimum Dst value to be in the earlier part of the 4-day time window. The minimum Dst value selected for each CME decides its geo-effectiveness according to the definition: Halo CMEs followed by $Dst < -50$ nT are considered geo-effective, to be consistent with most of the other works. We also regard halos followed by $Dst < -100$ nT as strongly geo-effective, while those followed by -50 nT $< Dst < -100$ nT as moderately geo-effective.

6. Result and Discussion

Several physical relationships have been investigated to select geo-effective CMEs such as CME angular width, CME location and speed, magnetic field orientation of a CME's source region and a CME earthward direction parameter. Year wise speed distribution of all CMEs shows highest average speed 386 km/s and lowest average speed 267 km/s which belongs to year 2012 (period of high solar activity) and 2008 (year of solar minima in rising phase of cycle 24), respectively. Considering all geo-effective CMEs (front and back sided), average and median speeds are 1183 and 996 respectively which shows the correlation between CME speed and geo-effectiveness. The Front side disk halos corresponds to the highest average and median speeds (~ 1517 km/s and 1502 km/s resp.) while the lowest average and median speeds (826 km/s and 804 km/s resp.) belongs to Backside limb halos. Most of the geomagnetic storms events comprise between CME speeds 500 km/s to 2000 km/s. It is noted that front side halos are faster than back side halos (having speed below 1500 km/s). Speed distributions for Front side disk halos and Front side back halos are somehow similar except small tail (between 2000 to 2500 km/s) in backside halo. At starting CME Speeds (<500 km/s), the number of GE events are very less but at speed 600 to 1000 km/s the number of GE events are maximum for front side halos and after that as the speed increases no. of event decreases. About 48% limb halo CMEs are geo-effective. Geomagnetic activity is found to be larger during the period of high solar activity i.e. most of the GE (geo-effective) halo CMEs are found in maximum phase of solar activity. All front side limb halos during the year 2011 are found to be geo-effective while rate of geo-effectiveness was 29% for F side disk halo. As expected rate of geo-effectiveness for back side halos is very low $\sim 15\%$. Taking into consideration 11 strong geo-effective storm ($Dst < -100$ nT) it has been found that 75% storm are due to Front side halos also 83% from them are limb halos. Also, it has been noted that $\sim 60\%$ of geo-effective CMEs are from West hemisphere which is in agreement with the earlier studies. We have also studied distribution of Dst values for different types of Halo which shows highest average and median Dst value (-84 nT and -74 nT respectively) belongs to Front side Limb Halos which is nearer to the range of strong storm while random sample shows -50 nT and -26 nT for average and median (respectively) which fall in the range of weak storm.

Severe storms ($Dst < -200$ nT) not have been observed during the initial phase of solar cycle 24. Such type of storms were presented on all earlier cycles (with complete Dst data), as studied by other researchers. Also, there have been twice intense storm ($Dst < -100$) in the similar period of solar cycle 23. The lower rate of geo-effectiveness of CMEs found as compare to studies of earlier solar cycle by other researcher is somehow as per prediction since the rate of geo-effective storm days (as defined by NOAA G-storm sizes) during the rising phase of each solar cycle is approximately correlated with the peak SSN in the solar cycle. If extrapolate this relationship, the lower rates can be found in solar cycle 24, (Figure- 3) they suggest values for the peak SSN in solar cycle 24 that consistent with the NOAA SWPC prediction which indicate that this solar cycle

24 is likely to be the weakest cycle since 1932. It should be also noted that the CME observed at STEREO A in July 2012 with southward magnetic fields reaching ~ 45 nT might have produced very intense storm if had encountered the Earth. So, the unusually weak levels of geomagnetic activity existing during the rise of cycle 24 do not imply that extraordinarily strong storms are unlikely to occur during this cycle.

References

[1] N. Gopalswamy, A. Lara, S.Yashiro, S.Nunes, and R.A. Howard, coronal mass ejection activity during solar cycle 23, Proc. ICS 2003 Symp., Eur. Space Agency Spec. Publ., E SA-SP 535, p.403(2003a) .
 [2] N. Gopalswamy, The Sun and the Heliosphere as an Integrated system, chap. 8, p. 201-252, edited by G. Poletto and S.T. Suess, Kluwer Acad., Bostan, 2004.
 [3] O.C. St. Cyr et al., Properties of Coronal mass ejections: SOHO LASCO observations from January 1996 to June 1998, J. Geophys. Res., 105, p.169, 2000.

[4] X.P., Zhao, and D.F. Webb, Source regions and storm effectiveness of frontside full halo coronal mass ejections, J. geophys. Res, 108 (A6), 1234, doi:10.1029/2002 JA009606, 2003.
 [5] M.M.S. Tiwari, and P.K., Shrivastava, Characteristic features of geomagnetic storms and their long term relationship with sunspot solar activity cycle, Ultra Science., 16(3), p329-334, 2004.
 [6] Nat Gopalswamy, , **61**, 1–3, 2009.
 [7] B. Mishra International Journal of Emerging Technologies in Computational and Applied Sciences, 5(6), June-August, 2013, pp. 557- 560.
 [8] Ian G. Richardson, J. Space Weather Space Clim. 3 (2013) A08.
 [9] David F. Webb et al., Living Rev. Solar Phys., 9, (2012), 3.

Figure Captions

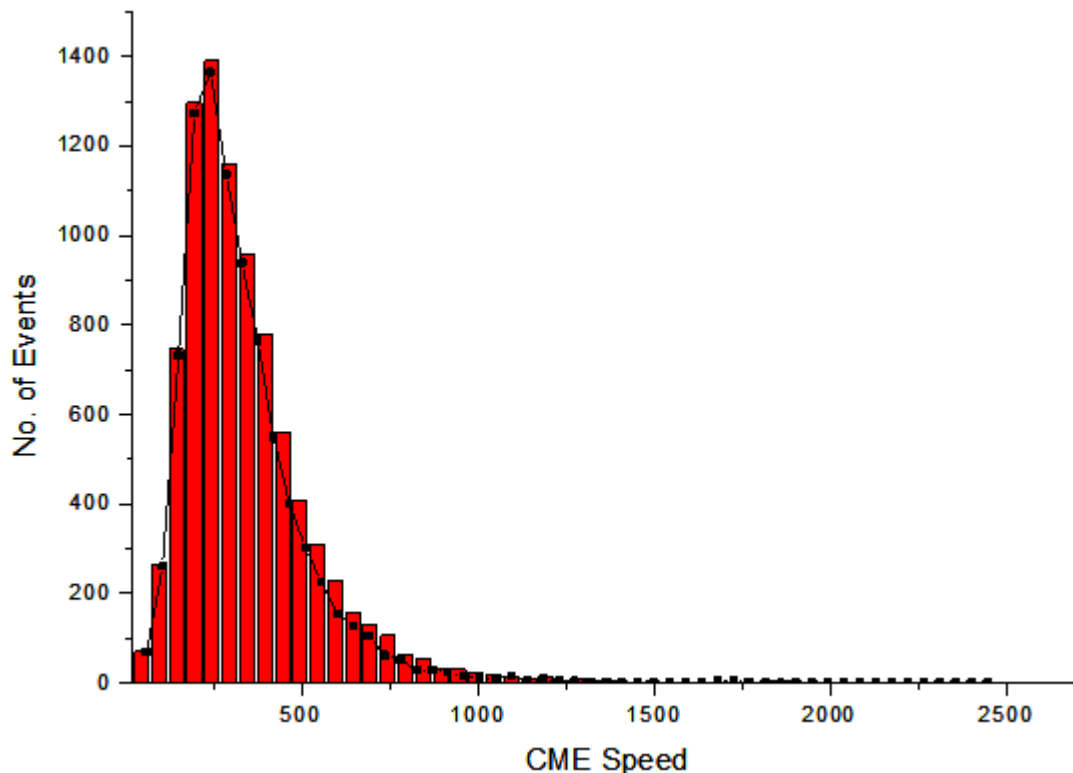


Figure 1: speed distribution for CME events during year 2008-2013 shows the distribution of the number of CMEs, N against their speeds . A strong peak at 344 km/ s and a long tail (>1000 km/s) to a good approximation that they can be fitted with a single log-normal distribution]

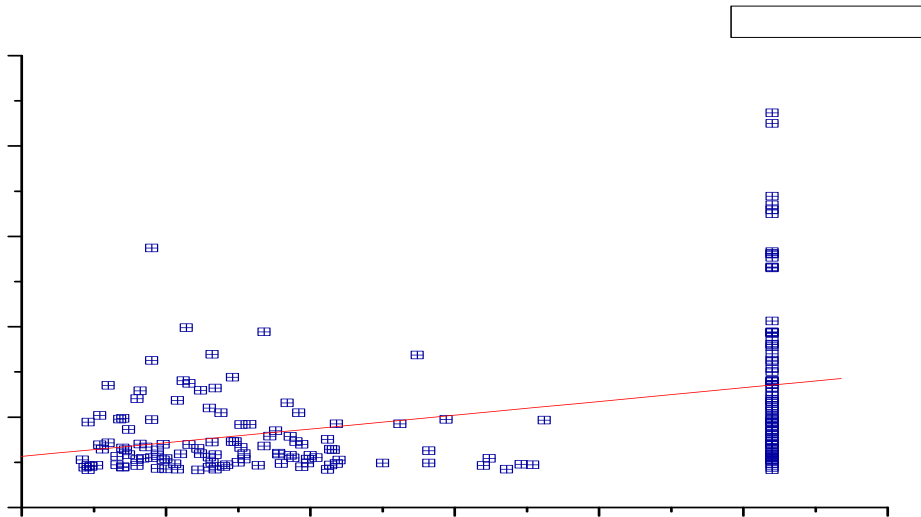


Figure 2: Graph showing relationship between CME Speed (> 700) and Angular Width with correlation coefficient $r = 0.40245$

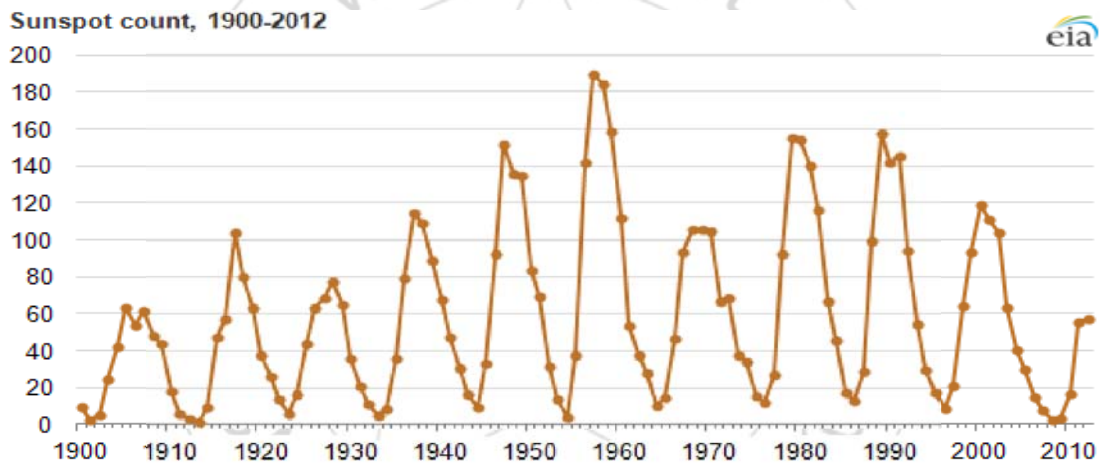


Figure 3: Yearly mean SSN / year, from 1900 to 2012, encompassing the rising phase of solar cycle 14 to the rise of cycle 24. The lowest rates during this period occurred in the minimum between cycles 23 and 24. The rate during the rise phase of cycle 24 is also lower than in any comparable interval during the period in this figure. Even 6 years into solar cycle 24, the storm rate is still only comparable to, or less than, the rates in the minimum activity years of previous cycles. (Source – NASA)]